Published in final edited form as:
Biochemistry. 2013 June 4; 52(22): . doi:10.1021/bi301519p.

Matrix-Assisted Laser Desorption Ionization Imaging Mass Spectrometry: In Situ Molecular Mapping

Peggi M. Angel[†] and **Richard M. Caprioli**[‡,*]

[†]Mass Spectrometry Research Center and Department of Biochemistry, Vanderbilt University Medical Center, 465 21st Avenue South, MRB III Suite 9160, Nashville, Tennessee 37232, United States

[‡]Mass Spectrometry Research Center and Department of Biochemistry, Medicine, Pharmacology, and Chemistry, Vanderbilt University Medical Center, 465 21st Avenue South, MRB III Suite 9160, Nashville, Tennessee 37232, United States

Abstract

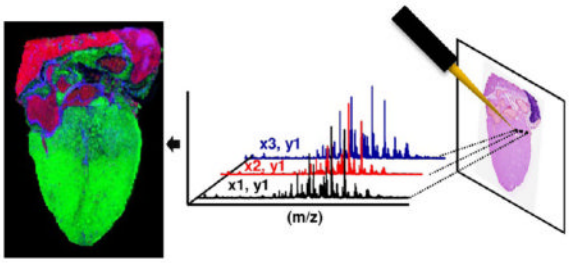

Matrix-assisted laser desorption ionization imaging mass spectrometry (IMS) is a relatively new imaging modality that allows mapping of a wide range of biomolecules within a thin tissue section. The technology uses a laser beam to directly desorb and ionize molecules from discrete locations on the tissue that are subsequently recorded in a mass spectrometer. IMS is distinguished by the ability to directly measure molecules in situ ranging from small metabolites to proteins, reporting hundreds to thousands of expression patterns from a single imaging experiment. This article reviews recent advances in IMS technology, applications, and experimental strategies that allow it to significantly aid in the discovery and understanding of molecular processes in biological and clinical samples.

Imaging mass spectrometry (IMS) dates back to the early 1960s when secondary ion mass spectrometry (SIMS) was developed to generate images of the distribution of Al, Mg, and Si on the surface of a solid sample substrate.[1] The use of SIMS for imaging of biological tissue was reported in the 1970s for imaging elements and low-molecular mass compounds such as lipids, drugs, and fragments of molecules.[2,3] Matrix-assisted laser desorption ionization (MALDI) MS was introduced in the mid-1980s[4,5] and was shown to be able to measure intact masses of a wide molecular mass range of biological molecules. Subsequently, MALDI MS was employed in an imaging mode to map on-tissue biochemistries and ion distribution maps of peptides and proteins across thin sections from rat pituitary and pancreatic tissues.[6] Since these initial imaging experiments, new technological advances and

[*]Corresponding Author: Vanderbilt University School of Medicine, 465 21st Ave. S., MRB III Suite 9160, Nashville, TN 37232. Telephone: (615) 343-2712. Fax: (615) 343-8372. r.caprioli@vanderbilt.edu.

The authors declare no competing financial interest.

sample preparation protocols have been developed that permit high-spatial resolution images to be produced with the molecular fidelity offered by mass spectrometry. Over the intervening years, other mass spectrometric imaging approaches have been reported such as desorption electrospray ionization (DESI) and laser ablation–inductively coupled plasma (LA-ICP) analysis.[7] However, in this work, we focus on current MALDI IMS strategies and highlight recent applications used to investigate the molecular complexity of biological tissues through their spatial distribution in both the healthy and diseased states.

MALDI MS provides a rather unique imaging platform because of its molecular specificity and the fact that the analyte itself is ablated, ionized, and detected directly from the tissue. Thus, it is ideal for discovery because no target specific reagents, such as antibodies, are needed. Further, many hundreds of analytes in the tissue are imaged simultaneously, providing analysis of a wide range of compounds in a multiplex image analysis. Because homogenates and extracts are not used to produce images, high local concentrations of analytes can be observed that might otherwise be lost in an assay that averages concentrations of analytes through extraction of relatively large areas of tissue.

Classically, spatial information from biological processes in tissue has been obtained from techniques such as histology staining, immunohistochemistry, and in situ hybridization. However, the first method is not molecularly specific, and the latter two require knowledge of the target analyte before investigation and are limited to simultaneous investigation of only a few analytes at one time. In addition, these methods often lack specificity for molecules such as drugs and their metabolites, lipids, protein isoforms, and mutations, post-translational modifications, and products of protein cleavage.

An overview of the IMS process for molecular mapping is shown in Figure 1, exemplified for the imaging of a section of an adult mouse heart “preserved through flash freezing”. Thin tissue sections cut on a cryostat are coated with a chemical matrix to facilitate laser energy desorption and ionization of molecules from within the tissue. Following ablation of multiple spots on the tissue by the laser, each ablated spot or pixel is correlated with a specific *x*,*y* coordinate in the tissue. The size and pitch of the pixels determine the final spatial resolution of the image. The mass spectrum from each pixel reports intensity versus mass-to-charge ratio of thousands of ions. Selecting an ion from the mass spectrum and plotting its intensity over all the pixels produces a map of that ion across the sampled area. Comparison between the IMS image and histological stained microscopic image often allows one to determine molecular patterns relative to anatomical structure within the tissue.

Spatial information using IMS may also be obtained by “histology-guided” molecular profiling. Here, regions marked by a biologist or pathologist on a serial section of stained tissue are overlaid onto the tissue mounted for IMS experiments. Enzymes and matrices may be placed with a high degree of accuracy and precision on the defined spot, usually robotically.[7] Thus, the goal of this approach is to produce mass spectra from carefully defined areas or spots on the tissue evaluated through the experience of investigators. Entire images are not required in this approach, thus saving acquisition time, giving smaller data file sizes, and providing spatially targeted information.

EXPERIMENTAL CONSIDERATIONS

A typical experimental approach to acquiring ion images by IMS is shown in Figure 2. Results from an IMS experiment are dependent on a number of parameters, including sample collection and preparation, instrumentation, and data processing. These parameters are interactive and ultimately play a major role in the quality of the final images produced. Careful planning is essential and ideally should occur before sample collection. The

experiment begins with determination of the biological question to be answered and the class of analyte (e.g., drug metabolite, lipid, peptide, or protein) to be analyzed. The minimal required spatial resolution of the images to be produced, sufficient to answer the biological question, is determined, as this affects other steps in the experiment. Lower spatial resolutions (75–200 μm) are useful for analysis of large samples such as an intact organ, e.g., a rat brain with dimensions of 10 mm × 12 mm, or even a whole mouse or rat body section. Moderate spatial resolution (10–75 μm) allows targeting of small anatomical substructures, and the highest spatial resolution (≤10 μm) is used for studies at a cellular level. As the spatial resolution increases, the sensitivity decreases because of the smaller area being ablated, data acquisition times increase, and larger data files are produced. Consequently, computational resources for analysis and storage of the data postimaging must be considered especially with large data sets that are associated with high-spatial resolution imaging of large sample areas. Basically, it is beneficial to choose the lowest spatial resolution possible that gives the required information to solve the biological problem being investigated.

Sample Collection

Samples must be preserved from the point of collection in the orientation needed for the imaging experiment because disrupted tissue morphology may lead to ambiguous or misinterpreted results. Often, how the sample is preserved determines the types of analytes that can be imaged. For instance, the vast banks of formalin-fixed paraffin-embedded (FFPE) tissues are limited mainly to peptide analysis from on-tissue protease digestions because of chemical cross-linking used in the fixation process. In addition, FFPE fixation leads to at least partial loss of some analytes such as metabolites, lipids, and drugs. Fresh frozen tissue provides the widest range of experiments and allows all analytes to be imaged. Tissue embedded in Optimal Cutting Temperature medium (OCT) should be avoided because it requires additional sample preparation steps for the removal of the surface polymer that can interfere with the analysis of the analytes. Specific preparation protocols provide alternate embedding media for use in IMS experiments.[8,9] Preserved tissue is sectioned by microtome at 5–6 μm for FFPE or by cryostat at 3–12 μm for fresh frozen or embedded tissue. When using instruments that have high voltage ion sources such as MALDI TOF instruments, tissue sections should be mounted on conductively coated surfaces such as gold-coated MALDI target plates, stainless steel plates, or ITO-coated microscope slides to prevent the buildup of charge on the sample during analysis. Modern imaging software supports the coregistration of stained or IHC sections with the MS image data, and the use of ITO-coated microscope slides facilitates histology staining and recording of the same section. This can be done upon completion of the imaging experiments to allow more precise matching of the histological and MS images. Stained sections serial to the imaged section can also be used to mark regions of interest for selected areas of analysis. Neighboring adjacent sections may be used for additional IHC stains.

Sample Preparation

Specific sample preparation protocols depend on the application to be studied. Tissue sections are typically washed after they are mounted on the sample target. For proteins, organic washes are used to fix the tissue to the target and remove lipids that may suppress the protein signal.[10] Aqueous washes are used to remove salts prior to lipid analysis to achieve the highest sensitivity.[11] A chemical matrix is then applied across the area to be analyzed; MALDI matrices are generally low-molecular mass acidic organic molecules that absorb laser energy to facilitate ablation and ionization of the analyte. Common matrices are sinapinic acid (SA) for protein analyses, 2,5-dihydroxybenzoic acid (DHB) for lipid analyses, and α-cyano-4-hydroxycinnamic acid (CHCA) matrix for peptide analyses, but many more have been reported.[12,13] The method of matrix application will determine the

attainable spatial resolution. Robotic spotting provides low spatial resolution (150–200 μm spot sizes) and efficient analyte extraction.[14] Automated spraying[15,16] and sublimation[17] are high-throughput processes for application of a homogeneous coating for low- to high-spatial resolution imaging. Manual spraying of matrix is a low-cost process but is subjective and often difficult to reproduce. Matrix may also be applied as a precoating before the tissue is mounted onto the target.[18] Strategies for multiple analytes may be used to increase the range of biomolecular information and obtain simultaneous information about lipids, peptides, and proteins.[18,19] It is not uncommon for investigations to develop customized sample development prior to data acquisition.

Instrumentation

There are many instrument configurations that may be used to collect IMS data. Nearly any MALDI mass spectrometer may be used to perform IMS experiments if equipped with an *x*,*y* movement sample stage of high precision. Two major factors determine the resolution: the laser spot size on the target and the pitch of the spots across the tissue in the ablation array. Current commercial instruments are equipped with lasers that may be attenuated to routinely reach laser spot sizes with ≥20 μm diameters with acquisition rates of 1000 Hz. An alternate approach to obtaining higher-spatial resolution images is to use an oversampling technique. Here, the laser spot is positioned to overlap between adjacent spots so that the derived signal originates from only a fraction of the original laser spot size.[20] This technique is useful when the beam size cannot be attenuated to reach a desired smaller spot size, but complete sample ablation of each spot is necessary to obtain reasonable results.

Specificity for a target analyte is determined by the mass analyzer. Linear time-of-flight analyzers are used to image approximately 3 to >50 kDa proteins. In some cases, careful sample preparation and special tuning of the instrument can result in the measurement of protein signals up to 250 kDa from biological tissue.[21] As *m*/*z* decreases, greater molecular specificity (i.e., higher mass resolution) is needed due to chemical interference from background signals and an increasingly complex population of near-isobaric or nominally isobaric masses. The reflectron TOF provides higher resolving power relative to that of a linear TOF for analysis of molecules from several hundred to approximately 3 kDa, covering the mass range for peptides and lipid imaging on-tissue. For small molecules in the range of a few hundred daltons, tandem mass spectrometry (MS/MS) or gas phase ion mobility instruments can be of great value. Common analyzers for MS/MS imaging are the ion trap, TOF/TOF, and QTOF instruments used for small molecule imaging.[22] Typically, images are produced by selection of a fragment ion transition from the parent ion, i.e., where only ions of intact mass M1 (parent ion) fragment to mass M2 are measured (M1 $\rightarrow$ M2). This is also known as single-reaction or selected reaction monitoring (SRM). Ion mobility analyzers separate ionized molecules generated from complex samples on the basis of gas phase mobility, dependent on the ion's charge, size, and shape (collisional cross section) as well as the type of carrier gas.[23] Isobaric species may thus be separated on the basis of gas phase ion structure. Both MS/MS and ion mobility analyzers greatly minimize interference from the chemical background. Finally, MALDI coupled to high-mass accuracy instrumentation such as an orbital ion trap or a Fourier transform ion cyclotron resonance (FT ICR) analyzer can provide data with mass accuracies of 0.1–5 ppm and resolving powers of ≥150000. Because of atomic mass defects, ions of the same nominal mass, but different exact mass, may be distinguished and imaged separately.[24,25]

Current improvements in instrumentation focus on increasing spatial resolution to achieve single-cell imaging and increase speed of analysis. Multiple approaches have been devised to target single-cell images. A recent advance in targeting single cells for IMS utilize a transmission geometry vacuum ion source in which the laser irradiated the back side of the

sample on a glass slide through a microscope objective. This allows simultaneous sample viewing for targeting and analysis, for example, producing distinct images of lipid patterns within HEK-293 cells at a 1 μm lateral resolution.[26,27] In another report, single cells were targeted for imaging analysis by equipping the source chamber with a CCD camera to capture optical images with separated ion optics utilizing a defocused triplet lens to limit the laser spot size.[28] This mass microscope showed localization of lipids to single-cell layers of salamander retina.[29] An additional study showed the use of an atmospheric-pressure MALDI source coupled to an orbital ion trap for accurate mass imaging of HeLA cells at a 7 μm lateral resolution, correlating with optical fluorescence images.[30,31]

Advances in instrumentation have made significant progress toward achieving simultaneous high spatial resolution and high-speed imaging. A high-speed MALDI TOF MS instrument with laser repetition rates of up to 5 kHz and a continually scanning stage of up to 10 mm/s produced images of rat brain (30 mm × 5 mm) in <10 min.[32] In another report, a novel chevron multichannel plate (MCP) detector capable of resolving both position and time-of-flight information was coupled to a TOF ion microscope to collect pixels of 740 nm × 740 nm from mouse testis.[33] The potential for collecting the entire mouse testis (5.4 mm × 5.4 mm) was estimated at 23 min, limited by the rate of transfer of data to the computer. These instruments show a strong potential to routinely achieve cellular level imaging within minutes and represent prototypes of the next generation of imaging MS instruments.

Data Processing

Data processing and analysis are essential for reliable interpretation of IMS results and have become an integral part of the IMS experiment through computational advances. After the collection of imaging data, individual MS spectra are processed by smoothing and background subtraction, supported by both open-source [BioMap (http://www.maldi-msi.org)] and commercial software. Normalization is used to minimize noise and variation across the entire sample caused by sample preparation. The most commonly used normalization procedure adjusts all pixels relative to the total ion current.[34] Newly developed methods normalize to a selected peak or a mass window, by root means square, or to the median of all signal intensities.[35,36] Normalization is evaluated on a case-by-case basis to determine which method produces ion patterns following histology without introducing noise-related expression patterns.[35] Commercial software packages now provide an assortment of normalization strategies, along with coregistration of multiple optical images to aid in interpreting normalization procedures.

Within the past 5 years, there have been significant improvements in the statistical evaluation of IMS data. Clinically oriented investigations utilize multivariate analysis and classification algorithms to determine molecular signatures correlating to prognosis or diagnosis.[37–40] An in-depth review of the evaluation and use of statistical testing for imaging mass spectrometry, including clinically relevant topics, has been published.[41] Advances in computational data reduction and refinement have led to significant progress in the pursuit of high-speed processing and analysis of large data sets from lipid, peptide, and protein IMS experiments.[42,43] Continued computational advances are important for obtaining accurate and robust expression visualization and for statistical evaluation of ion image patterns from IMS studies.

PHARMACEUTICALS AND METABOLITES

IMS has been widely used as a method to study target tissue dosing, drug degradation and metabolism, and colocalization with other biomolecules throughout multiple organs.[44] Extensive pretreatment and washing of the tissue are avoided, because this may delocalize or deplete the analytes in the tissue. The specific MALDI matrix used is chosen and

optimized for sensitive and specific detection of the analyte in either positive or negative ion mode mass spectrometry and to limit interference from matrix peaks. MS/MS imaging for single-reaction monitoring[22] or multiple-reaction monitoring (MRM),[45] and ion mobility,[46] increase the specificity of detection in the presence of chemical noise and isobaric to near-isobaric peaks from other compounds. An example is shown in Figure 3, where the distribution of sinalbin on *Noccaea caerulescens* tissue was only accomplished using SRM imaging. Sinalbin, a glucosinolate, was detected with higher concentrations in new leaflets, correlating with the known protective role of sinalbin for new leaflets. Other means of enhancing the sensitivity for a given analyte may be achieved by chemical derivatization combined with optimized sample preparation protocols.[46,47]

Several investigators have focused on obtaining quantitative information from images and subsequent correlation with LC–MS/MS studies.[22,45,47] For example, MRM imaging was employed to investigate moxifloxacin dosing in a rabbit model of lung tuberculosis.[45] Levofloxacin was homogeneously sprayed onto the tissue as a reference standard for image normalization. Images from MS/MS analyses for moxifloxacin showed reproducible levels of the drug, with the highest levels in granulomatous lesions and lower levels in necrotic cores and across the entire lung. Quantification of moxifloxacin at postdosing intervals closely correlated to LC–MS/MS studies.

Imaging of whole body tissue sections facilitates simultaneous relative quantitation of pharmaceuticals and their metabolites colocalized with endogenous compounds such as proteins and lipids throughout many organs.[46,48] This technology may be used for uncovering novel metabolites and measuring their clearance from multiple organs without prior knowledge of their metabolism. A recent study utilized an accurate mass defect filtering method for detection of reserpine, an antihypertension and psychosis drug, and discovery of the unexpected metabolic distribution of reserpine throughout whole body (WB) sections.[49] These experiments used a high-mass resolution instrument to collect accurate mass information for reserpine within dosed rats. Common reserpine metabolic pathways, including oxygenation/reduction or sulfation and glucuronidation, were used to predict the 50 most likely metabolites. Postprocessing of imaging data used mass defects to isolate reserpine metabolites on the basis of predicted chemistries, and these were confirmed by MS/MS experiments.

Another interesting area of application of IMS is the study of drug-eluting medical implants and the investigation of in situ pathology around implanted devices. Recently, IMS studies of sirolius, an antistenotic drug, from drug-eluting coronary stents found an in situ gradient of sirolius along the length of the stent 14 days after implantation, as well as multiple degradation products after 8 days under stressed conditions.[50] In another study, the release of theophylline, a drug for chronic obstructive pulmonary disease, among other drugs, from novel lipid implants was measured with subsequent construction of a mathematical model for drug formulation.[51]

LIPIDS

The enormous complexity of possible lipid structures, estimated at hundreds of thousands,[52] is generally confined within a narrow *m*/*z* range spanning approximately 300–4500. Whereas there are very few reagents that recognize specific lipid species, IMS can map the localization of hundreds of individual lipid species in one experiment. MS/MS approaches can be used to identify lipids from the same tissue section.

IMS of lipids is generally performed on fresh frozen tissue, as other preservation processes deplete the lipid population. Commercially available frozen embedding media may be used

but often require extra sample preparation to remove the embedding media that may produce contaminant peaks interfering with the analyte signal. To increase the magnitude of the lipid signal and simplify data interpretation and processing, tissue sections may be washed with aqueous buffers.[11] The choice of buffer should be made with care because it may affect sensitivity. Figure 4 shows an example of lipid imaging on a section of a mouse embryo at embryonic day 13.5, mapping different lipid classes and products of lipid saturation to the developing organs. This image was acquired at 20 μm spatial resolution and is shown as an overlay of four individual lipid species.

Positive and negative ionization modes should be tested with different matrices because different lipid classes ionize preferentially in positive mode versus negative ion mode. Dry matrix applications, which prevent lipid delocalization,[17,53] allow the acquisition of images with spatial resolutions limited only by laser spot size. As with pharmaceuticals and other metabolites, ion mobility[46] and MS/MS imaging[22,54] are used to increase the specificity for lipid peaks. Instruments with high resolving power and high mass accuracy have proven to be especially useful for the field of lipid imaging, resolving the multiple near-isobaric peaks and their isotopic envelopes within complex lipid populations.[55]

The use of IMS for lipid research has become more common with the knowledge that this technology provides both spatial localization and identification of lipids. For example, IMS was used to investigate phospholipids in normal mouse lung tissue where an unexpected increase in localized concentrations of arachidonate and docosahexaenoate phospholipids was discovered within the lung tissue.[9] These polyunsaturated fatty acid-containing phospholipids were found localized to airway edges marked by immunohistochemistry. Additionally, sphingomyelins were found in edges of lung blood vessels and known lung surfactant lipids, both glycerophosphocholines and glycerophosphoglycerols, mapped to lung alveoli, corresponding to localization of stored lung surfactants.

In terms of clinical and translational studies, lipid alterations were measured in symptomatic great saphenous veins collected from varicose vein patients versus control veins.[56] The accumulation of lipid in the great saphenous veins is thought to precede veinous valvular dysfunction. Results from a small patient cohort revealed an abnormal distribution and an increase in levels of several glycerophosphocholines and triglycerides in varicose veins in contrast with those in control veins. The study implied that the accumulation of lipid begins in early stage varicose veins and may lead to chronic inflammation and subsequent tissue degeneration around affected areas.

Another report examined the lipid composition of the breast tumor microenvironments, as the lipid composition of tumors has been associated with tumor metastatis.[57] MDA-MB-231 cells were injected into athymic nude mice and monitored until the tumor size reached 500 mm^3. Positive ion mode imaging performed by ion mobility mass spectrometry produced information about the localization of acylcarnitine, lysophosphocholines, sphingomyelins, and glycerophosphocholines within the tumor. Relative quantification revealed a uniquely altered lipid signature of glycerophosphocholines, sphingomyelins, and acylcarnitines between tumor regions. Here, imaging by ion mobility eliminated matrix-related ions from the imaging analysis and allowed detection of less abundant acylcarnitines.

PEPTIDES

Imaging of peptides in tissue has been successful in mapping both endogenous peptides and those produced from in situ enzymatic digestion. Enzymatic digestions allow proteomic analysis of FFPE tissue where proteins are cross-linked and may also be used to access high-

molecular mass proteins (>50 kDa) that can be difficult to analyze intact without extensive sample preparation and instrumental tuning.

Although huge stores of FFPE tissues exist in clinical repositories worldwide, imaging of intact protein is not practical because of cross-linking from chemical fixation. However, antigen retrieval techniques coupled with in situ tryptic digestion on the tissue release peptides that are not cross-linked and may subsequently be sequenced by MS/MS directly off of the tissue.[7] Established protocols for protein database queries subsequently identify the nominal protein by matching to the peptide sequence tags obtained from the tissue.

A major use of peptide imaging with FFPE tissues is the discovery of molecular markers associated with disease diagnosis or progression in clinical biopsies. FFPE tissue is often available in a tissue microarray (TMA) format and allows rapid high-throughput analysis from large clinical cohorts.[58] Peptide signatures from TMAs are used to determine the biological alteration of proteins that mark a disease state and may be used to classify disease states and early markers of disease.[58,59] Figure 5 shows an example of peptide classification using the molecular signature from a TMA made of cores from matched normal tissue and tissue diagnosed with clear cell renal carcinoma.[60] After the TMA section is mounted on a target, the cores are treated with trypsin to release cross-linked peptides. An optical image of a serial section stained with H&E is used to mark regions of interest to the pathologist. The cores on the target are imaged, and through biocomputational processing, molecular signatures of disease and normal states are produced. These signatures, after validation, are used in the high-throughput screening of additional biopsies.

Often the molecular signature derived from the tissue is more accurate in distinguishing disease states that may not be apparent by pathology grading. As an example, a Spitz nevus, a benign skin lesion, and Spitzoid, malignant melanoma were examined by IMS to identify proteomic differences.[38] These skin lesions are sometimes difficult to diagnose by pathology. Melanocytes from 114 FFPE-preserved archival specimens were marked by a pathologist, followed by peptide IMS profiling. Statistical modeling revealed a signature of five peptides that were able to distinguish between the benign and malignant state with a sensitivity and specificity of ≥90%.

Endogenous peptide signatures can be obtained from fresh frozen tissue. Tissue sections are treated by alcohol-based washes, as in intact protein imaging.[10] Other washes must be used with caution so as not to deplete more hydrophilic peptides. Common MALDI matrices for endogenous peptide imaging include CHCA and DHB applied by either precoating[18] or postcoating methods. Endogenous peptide imaging has been reported for investigation of opioid peptides in a rat model of L-DOPA-induced dyskinesia in Parkinson's disease.[61] Fresh frozen tissue from L-DOPA treatments spanning 15 consecutive days was robotically spotted with a DHB solution and analyzed via IMS. Unique expression patterns of endogenous opioid peptides in striatal tissue lesions could be correlated with increased dyskinesia and included higher levels of neuropeptides dynorphin B, α-neoendorphin, and substance P. Dynorphin B and α-neoendorphin had a positive correlation with the severity of L-DOPA-induced dyskinesia, corresponding to previous reports involving mRNA expression. Novel non-opioid receptor-mediated changes in the striatum of dyskinetic rats were implicated.

Recently, MRM experiments have been conducted to explore quantitation of peptide expression produced by the on-tissue tryptic digest of fresh frozen rat brain.[62] After tryptic digestion, an isotopically labeled peptide was robotically sprayed onto the tissue, followed by MALDI matrix application. On-tissue calibration curves generated from analysis of isotopically labeled standards applied over a range of concentrations showed a good

correlation between the amount applied and signal intensity. However, ongoing challenges for absolute quantification of an on-tissue peptide include the ability to identify and use peptides that are unique to a protein, the development of standard methods, including normalization procedures, and the evaluation of the accuracy of the quantification measurement across different types of tissues.

PROTEINS

Intact protein imaging by IMS can produce distribution patterns of proteins, protein isoforms and mutations, post-translational modifications, and products of protein cleavage or degradation. Protein identification strategies are applied separately from the IMS experiment, although there has been significant progress in fragmenting intact proteins directly from tissue. Currently, large peptides and some low-molecular mass proteins (<18.5 kDa) can be identified intact directly from the tissue.[63,64] Higher-molecular mass proteins must be digested to peptides for identification, either in situ or in a subsequent experiment using a protein extract from tissue.

There are many approaches that have been developed to access protein content from tissue for IMS experiments. Several protocols have been established for ethanol fixation of proteins, allowing reproducible orientation of tissue and collection of tissue sections targeting a region of interest without cross-linking protein structure as in FFPE tissues.[65,66] The majority of intact protein imaging is performed on fresh frozen tissue treated with alcohol-based washes.[10] Aqueous washes have uncovered both modified and unmodified membrane proteins.[67,68] Altering the organic content of washes with optimized instrumental parameters expands the mass range of proteins observed from tissue.[69,70] Sinapinic acid is a commonly used matrix for protein analysis, and the addition of detergents to the matrix is sometimes employed to enhance protein signals.[71] Matrix sublimation protocols for protein analysis require rehydration with organic solvents to produce intense signals and achieve spatial resolutions of approximately ≥10 μm.[72] Figure 6 shows an example of protein imaging performed on a rat kidney prepared using matrix sublimation followed by rehydration. Rehydration with organic solvents has also been found to improve the signal from automated spray application of the matrix.[73]

Protein signatures from clinical tissue specimens have been obtained using IMS for improved diagnosis and prognosis.[64,74–76] For example, an investigation of a cohort of 38 biopsies from Barrett's adenocarcinoma was performed to improve the prediction of lymph node metastasis and disease outcome.[75] Hierarchical clustering of IMS protein signatures from selected regions revealed two clusters corresponding to either intestinal metaplasia or Barrett's adenocarcinoma. Six proteins, including S100-A10 (*m*/*z* 11185), COX7A2 (*m*/*z* 6720), and TAGLN2 (*m*/*z* 22262), were identified as potential markers for Barrett's adenocarcinoma. Validation by immunohistochemistry on a cohort of 135 biopsies revealed that strong expression of COX7A2 and TAGLN2 corresponded to poor prognosis. S100-A10 was an independent prognosticator, and patients with high expression levels showed significantly worse disease free survival than patients with low levels of expression of S100-A10.

Multimodality approaches have been used to understand multidimensional distributions of molecular signatures in disease,[77–79] and this topic has been reviewed recently.[80] As an example, a multimodality imaging study was employed to investigate the inflammatory response to *Staphylococcus aureus* infection in a rodent model using IMS and magnetic resonance imaging (MRI). MRI was used to monitor systemic inflammation due to a high soft tissue contrast and high spatial resolution and IMS was used to inform on innate immune protein recruitment in response to infection. *S. aureus* infection was induced in

mice by intravenous injection and at 4 days either treated with linezolid, an anti-inflammatory drug, or left untreated. The infection was allowed to proceed for an additional 4 days, resulting in treated animals with small abscesses or untreated animals displaying significant kidney abscesses with severe organ deformation. Besides other proteins, IMS data showed that calgranulin A, a subunit of calprotectin (*m*/*z* 10165), was most abundant at the sites of kidney abscesses. Coregistration of IMS data and MRI data showed that treated animals exhibited calprotectin expression at sites of kidney abscess, whereas untreated animals had an enhanced calprotectin signal in the entire organ, indicating that calprotectin is part of a robust inflammatory response during the formation of infectious abscesses in the murine kidney.

On-tissue chemistries targeting specific proteins, including high-molecular mass proteins, or protein activities have been reported.[81–83] These approaches apply laser labile tags to probes attached to target proteins within a tissue section. During IMS analysis, the tag is released, generating a map of target protein expression across the tissue. An activity-based probe was developed to monitor serine hydrolase activity on tissue.[83] The probe was bound to serine hydrolase on tissue sections incubated in phosphate-buffered saline, followed by chemical conjugation with a dendrimer carrying multiple laser labile tags. Upon irradiation by the laser, multiple tags were released in a single binding event, giving a multiplicative signal for increased sensitivity. This study showed the localization of serine hydrolase activity in developing hind limb and hind brain in a mouse embryo, as well as in corpus callosum and portions of the anterior commissure in an adult rat brain. Furthermore, recent work has illustrated that laser labile tags may be applied to multiple target proteins using short chain antibodies,[82] with the potential for future simultaneous imaging of many targeted proteins. A potential application for this would be the monitoring of protein pathways by IMS and correlation to biological processes.

CHALLENGES AND PERSPECTIVES

The current field of IMS has evolved to include an abundance of tools and strategies for the visualization of in situ molecular patterns from tissue. Continued efforts to improve sample preparation strategies and instrumentation will no doubt improve the capabilities for answering biological questions. For example, there is ongoing work to improve single cell imaging, rapid collection of high-spatial resolution data, and enhancement of sensitivity and specificity by both instrumental and sample preparation techniques. An increasing sensitivity and dynamic range represents an important area of development especially at high spatial resolution where there is little molecular material per pixel. Further, biocomputational challenges concomitant with increased spatial resolution include high data dimensionality and the development of more effective tools for data mining.

Integration of IMS with other imaging modalities is an area that shows enormous potential for increasing the amount of information obtained from biological tissues. IMS studies of human tissues show the impact and further potential of the technology for improving prognosis and diagnoses in clinical work. With continued development of the field, we believe that IMS will be utilized for routine, rapid evaluation of molecular processes in both biological and medical research. Further, we believe that this molecularly specific imaging technology can potentially provide critical information for the personalized care of patients.

Acknowledgments

Funding

This work was supported by grants from the National Heart, Lung, and Blood Institute (5RL1HL092551-05), the National Institute of General Medical Science (5R01 GM058008-14) and (8 P41 GM103391-02, formerly

5P41RR031461-02), from the National Institutes of Health. P.M.A. appreciates salary support by the National Center for Advancing Translational Sciences of the National Institute of Health via Grant UL1 TR000445.

ABBREVIATIONS

MALDI	matrix-assisted laser desorption ionization
IMS	imaging mass spectrometry
SA	sinapinic acid
CHCA	α-cyano-4-hydroxycinnamic acid
DHB	dihydroxybenzoic acid
SRM	selected reaction monitoring
FFPE	formalin-fixed paraffin-embedded
ITO	indium–tin oxide

References

1. Castaing R, Slodzian G, Dupouy MG. Optique Corpusculaire: Premiers essais de microanalyse par emission ionique secondaire. C R Seances Acad Sci. 1962; 255:1893–1895.
2. Galle P. Sur une nouvelle methode d'analyse cellulaire utilisant le phenomene d'emission ionique secondaire. Ann Phys Biol Med. 1970; 42:83–94.
3. Morrison GH, Slodzian G. Ion microscopy. Anal Chem. 1975; 47:932–943.
4. Karas M, Bachmann D, Hillenkamp F. Influence of the wavelength in high-irradiance ultraviolet laser desorption mass spectrometry of organic molecules. Anal Chem. 1985; 57:2935–2939.
5. Tanaka K, Waki H, Ido Y, Akita S, Yoshida Y, Yoshida T, Matsuo T. Protein and polymer analyses up to m/z 100 000 by laser ionization time-of-flight mass spectrometry. Rapid Commun Mass Spectrom. 1988; 2:151–153.
6. Caprioli RM, Farmer TB, Gile J. Molecular imaging of biological samples: Localization of peptides and proteins using MALDI-TOF MS. Anal Chem. 1997; 69:4751–4760. [PubMed: 9406525]
7. Casadonte R, Caprioli RM. Proteomic analysis of formalin-fixed paraffin-embedded tissue by MALDI imaging mass spectrometry. Nat Protoc. 2011; 6:1695–1709. [PubMed: 22011652]
8. Palmer AD, Griffiths R, Styles I, Claridge E, Calcagni A, Bunch J. Sucrose cryo-protection facilitates imaging of whole eye sections by MALDI mass spectrometry. J Mass Spectrom. 2012; 47:237–241. [PubMed: 22359334]
9. Berry KAZ, Li B, Reynolds SD, Barkley RM, Gijón MA, Hankin JA, Henson PM, Murphy RC. MALDI imaging MS of phospholipids in the mouse lung. J Lipid Res. 2011; 52:1551–1560. [PubMed: 21508254]
10. Seeley EH, Oppenheimer SR, Mi D, Chaurand P, Caprioli RM. Enhancement of protein sensitivity for MALDI imaging mass spectrometry after chemical treatment of tissue sections. J Am Soc Mass Spectrom. 2008; 19:1069–1077. [PubMed: 18472274]
11. Angel PM, Spraggins JM, Scott Baldwin H, Caprioli R. Enhanced Sensitivity for High Spatial Resolution Lipid Analysis by Negative Ion Mode Matrix Assisted Laser Desorption Ionization Imaging Mass Spectrometry. Anal Chem. 2012; 84:1557–1564. [PubMed: 22243218]
12. Thomas A, Charbonneau JL, Fournaise E, Chaurand P. Sublimation of new matrix candidates for high spatial resolution imaging mass spectrometry of lipids: Enhanced information in both positive and negative polarities after 1,5-diaminonapthalene deposition. Anal Chem. 2012; 84:2048–2054. [PubMed: 22243482]
13. Meriaux C, Franck J, Wisztorski M, Salzet M, Fournier I. Liquid ionic matrixes for MALDI mass spectrometry imaging of lipids. J Proteomics. 2010; 73:1204–1218. [PubMed: 20188221]
14. Aerni HR, Cornett DS, Caprioli RM. Automated acoustic matrix deposition for MALDI sample preparation. Anal Chem. 2006; 78:827–834. [PubMed: 16448057]

15. Prevost, TH.; Dwyer, JL. Nozzle arrangement for collecting components from a fluid for analysis. Lab Connections, Inc; Round Rock, TX: 1998.

16. Schuerenberg, M.; Deininger, SO. Chapter 7: Matrix application with ImagePrep. In: Setou, M., editor. Imaging Mass Spectrometry: Protocols for Mass Microscopy. Springer; Tokyo: 2010. p. 87-91.

17. Hankin JA, Barkley RM, Murphy RC. Sublimation as a method of matrix application for mass spectrometric imaging. J Am Soc Mass Spectrom. 2007; 18:1646–1652. [PubMed: 17659880]

18. Grove KJ, Frappier SL, Caprioli RM. Matrix pre-coated MALDI MS targets for small molecule imaging in tissues. J Am Soc Mass Spectrom. 2011; 22:192–195. [PubMed: 21472558]

19. Chughtai S, Chughtai K, Pastor BC, Kiss A, Agrawal P, MacAleese L, Heeren R. A multimodal mass spectrometry imaging approach for the study of musculoskeletal tissues. Int J Mass Spectrom. 2012; 325:150–160.

20. Jurchen JC, Rubakhin SS, Sweedler JV. MALDI-MS imaging of features smaller than the size of the laser beam. J Am Soc Mass Spectrom. 2005; 16:1654–1659. [PubMed: 16095912]

21. Chaurand P, Caprioli RM. Direct profiling and imaging of peptides and proteins from mammalian cells and tissue sections by mass spectrometry. Electrophoresis. 2002; 23:3125–3135. [PubMed: 12298084]

22. Reich, RF.; Garrett, TJ.; Magparangalan, DP.; Yost, RA. Distribution Studies of Drugs and Metabolites in Tissues by Mass Spectrometric Imaging. Vol. Chapter 14. Wiley; Hoboken, NJ: 2010.

23. Kiss A, Heeren RMA. Size, weight and position: Ion mobility spectrometry and imaging MS combined. Anal Bioanal Chem. 2011; 399:2623–2634. [PubMed: 21225246]

24. Cornett DS, Frappier SL, Caprioli RM. MALDI-FTICR imaging mass spectrometry of drugs and metabolites in tissue. Anal Chem. 2008; 80:5648–5653. [PubMed: 18564854]

25. Taban IM, Altelaar AF, van der Burgt YEM, McDonnell LA, Heeren R, Fuchser J, Baykut G. Imaging of peptides in the rat brain using MALDI-FTICR mass spectrometry. J Am Soc Mass Spectrom. 2007; 18:145–151. [PubMed: 17055739]

26. Zavalin, A.; Caprioli, R. Transmission Geometry Profiling/Imaging Mass Spectrometry with Sub-Cellular Resolution. 58th ASMS Conference on Mass Spectrometry and Allied Topics; Salt Lake City, UT. 2010.

27. Zavalin A, Todd EM, Rawhouser PD, Yang J, Norris JL, Caprioli R. Direct Imaging of Single Cells and Tissue at Subcellular Spatial Resolution Using Transmission Geometry MALDI MS. J Mass Spectrom. 2012; 47:1473–1481. [PubMed: 23147824]

28. Harada T, Yuba-Kubo A, Sugiura Y, Zaima N, Hayasaka T, Goto-Inoue N, Wakui M, Suematsu M, Takeshita K, Ogawa K. Visualization of volatile substances in different organelles with an atmospheric-pressure mass microscope. Anal Chem. 2009; 81:9153–9157. [PubMed: 19788281]

29. Lanni EJ, Rubakhin SS, Sweedler JV. Mass spectrometry imaging and profiling of single cells. J Proteomics. 2011; 52:463–470.

30. Koestler M, Kirsch D, Hester A, Leisner A, Guenther S, Spengler B. A high resolution scanning microprobe matrix-assisted laser desorption/ionization ion source for imaging analysis on an ion trap/Fourier transform ion cyclotron resonance mass spectrometer. Rapid Commun Mass Spectrom. 2008; 22:3275–3285. [PubMed: 18819119]

31. Schober Y, Guenther S, Spengler B, Rompp A. Single Cell Matrix-Assisted Laser Desorption/ Ionization Mass Spectrometry Imaging. Anal Chem. 2012; 84:6293–6297. [PubMed: 22816738]

32. Spraggins JM, Caprioli RM. High-Speed MALDI-TOF Imaging Mass Spectrometry: Rapid Ion Image Acquisition and Considerations for Next Generation Instrumentation. J Am Soc Mass Spectrom. 2011; 22:1022–1031. [PubMed: 21953043]

33. Jungmann JH, Smith DF, MacAleese L, Klinkert I, Visser J, Heeren RMA. Biological Tissue Imaging with a Position and Time Sensitive Pixelated Detector. J Am Soc Mass Spectrom. 2012; 23:1679–1688. [PubMed: 22836864]

34. Norris JL, Cornett DS, Mobley JA, Andersson M, Seeley EH, Chaurand P, Caprioli RM. Processing MALDI mass spectra to improve mass spectral direct tissue analysis. Int J Mass Spectrom. 2007; 260:212–221. [PubMed: 17541451]

35. Deininger SO, Cornett DS, Paape R, Becker M, Pineau C, Rauser S, Walch A, Wolski E. Normalization in MALDI-TOF imaging datasets of proteins: Practical considerations. Anal Bioanal Chem. 2011:1–15. [PubMed: 20967427]
36. Fonville JM, Carter C, Cloarec O, Nicholson JK, Lindon JC, Bunch J, Holmes E. Robust Data Processing and Normalization Strategy for MALDI Mass Spectrometric Imaging. Anal Chem. 2012; 84:1310–1319. [PubMed: 22148759]
37. Meding S, Nitsche U, Balluff B, Elsner M, Rauser S, Schöne C, Nipp M, Maak M, Feith M, Ebert M, et al. Tumor Classification of Six Common Cancer Types Based on Proteomic Profiling by MALDI Imaging. J Proteome Res. 2012; 11:1996–2003. [PubMed: 22224404]
38. Lazova R, Seeley EH, Keenan M, Gueorguieva R, Caprioli RM. Imaging Mass Spectrometry: A New and Promising Method to Differentiate Spitz Nevi from Spitzoid Malignant Melanomas. Am J Dermatopathol. 2012; 34:82–90. [PubMed: 22197864]
39. Schwamborn K, Krieg RC, Uhlig S, Ikenberg H, Wellmann A. MALDI imaging as a specific diagnostic tool for routine cervical cytology specimens. Int J Mol Med. 2012; 27:417–421. [PubMed: 21174066]
40. Jones EA, van Remoortere A, van Zeijl RJM, Hogendoorn PCW, Bovee JVMG, Deelder AM, McDonnell LA. Multiple Statistical Analysis Techniques Corroborate Intratumor Heterogeneity in Imaging Mass Spectrometry Datasets of Myxofibrosarcoma. PLoS One. 2011; 6:e24913. [PubMed: 21980364]
41. Jones EA, Deininger SO, Hogendoorn PCW, Deelder AM, McDonnell LA. Imaging Mass Spectrometry Statistical Analysis. J Proteomics. 2012; 75:4962–4989. [PubMed: 22743164]
42. McDonnell LA, Van Remoortere A, De Velde N, Van Zeijl RJM, Deelder AM. Imaging mass spectrometry data reduction: Automated feature identification and extraction. J Am Soc Mass Spectrom. 2010; 21:1969–1978. [PubMed: 20850341]
43. Jones EA, van Zeijl RJM, Andren PE, Deelder AM, Wolters L, McDonnell LA. High Speed Data Processing for Imaging MS-based molecular histology using graphical processing units. J Am Soc Mass Spectrom. 2012; 23:745–752. [PubMed: 22311727]
44. Prideaux B, Stoeckli M. Mass Spectrometry Imaging for Drug Distribution Studies. J Proteomics. 2012; 75:4999–5013. [PubMed: 22842290]
45. Prideaux B, Dartois V, Staab D, Weiner DM, Goh A, Via LE, Barry Iii CE, Stoeckli M. High-sensitivity MALDI-MRM-MS imaging of moxifloxacin distribution in tuberculosis-infected rabbit lungs and granulomatous lesions. Anal Chem. 2011; 83:2112–2118. [PubMed: 21332183]
46. Trim PJ, Henson CM, Avery JL, McEwen A, Snel MF, Claude E, Marshall PS, West A, Princivalle AP, Clench MR. Matrix-assisted laser desorption/ionization-ion mobility separation-mass spectrometry imaging of vinblastine in whole body tissue sections. Anal Chem. 2008; 80:8628–8634. [PubMed: 18847214]
47. Koeniger SL, Talaty N, Luo Y, Ready D, Voorbach M, Seifert T, Cepa S, Fagerland JA, Bouska J, Buck W. A quantitation method for mass spectrometry imaging. Rapid Commun Mass Spectrom. 2011; 25:503–510. [PubMed: 21259359]
48. Khatib-Shahidi S, Andersson M, Herman JL, Gillespie TA, Caprioli RM. Direct molecular analysis of whole-body animal tissue sections by imaging MALDI mass spectrometry. Anal Chem. 2006; 78:6448–6456. [PubMed: 16970320]
49. Shahidi-Latham SK, Dutta SM, Conaway MCP, Rudewicz PJ. Evaluation of an Accurate Mass Approach for the Simultaneous Detection of Drug and Metabolite Distributions via Whole-Body Mass Spectrometric Imaging (WB-MSI). Anal Chem. 2012; 84:7158–7165. [PubMed: 22827834]
50. Huang J, Hannah-Qiuhua L, Szyszka R, Veselov V, Reed G, Wang X, Price S, Alquier L, Vas G. Molecular imaging of drug-eluting coronary stents: Method development, optimization and selected applications. J Mass Spectrom. 2012; 47:155–162. [PubMed: 22359324]
51. Kreye F, Hamm G, Karrout Y, Legouffe R, Bonnel D, Siepmann F, Siepmann J. MALDI-TOF MS imaging of controlled release implants. J Controlled Release. 2012; 161:98–108.
52. Brown HA, Murphy RC. Working towards an exegesis for lipids in biology. Nat Chem Biol. 2009; 5:602–606. [PubMed: 19690530]

53. Puolitaival SM, Burnum KE, Cornett DS, Caprioli RM. Solvent-free matrix dry-coating for MALDI imaging of phospholipids. J Am Soc Mass Spectrom. 2008; 19:882–886. [PubMed: 18378160]
54. Burnum KE, Cornett DS, Puolitaival SM, Milne SB, Myers DS, Tranguch S, Brown HA, Dey SK, Caprioli RM. Spatial and temporal alterations of phospholipids determined by mass spectrometry during mouse embryo implantation. J Lipid Res. 2009; 50:2290–2298. [PubMed: 19429885]
55. Berry KAZ, Hankin JA, Barkely RM, Spraggins JM, Caprioli R, Murphy RC. MALDI Imaging of Lipid Biochemistry in Tissues by Mass Spectrometry. Chem Rev. 2011; 111:6491–6512. [PubMed: 21942646]
56. Tanaka H, Zaima N, Sasaki T, Yamamoto N, Sano M, Konno H, Setou M, Unno N. Loss of lymphatic vessels and regional lipid accumulation is associated with great saphenous vein incompetence. Journal of Vascular Surgery. 2012; 55:1440–1448. [PubMed: 22226181]
57. Chughtai K, Jiang L, Greenwood TR, Glunde K, Heeren RMA. Mass Spectrometry Images Acylcarnitines, Phosphatidylcholines and Sphingomyelin in MDA-MB-231 Breast Tumor Models. J Lipid Res. 201210.1194/jlr.M027961
58. Groseclose MR, Massion PP, Chaurand P, Caprioli RM. High-throughput proteomic analysis of formalin-fixed paraffin-embedded tissue microarrays using MALDI imaging mass spectrometry. Proteomics. 2008; 8:3715–3724. [PubMed: 18712763]
59. Bonnel D, Longuespee R, Franck J, Roudbaraki M, Gosset P, Day R, Salzet M, Fournier I. Multivariate analyses for biomarkers hunting and validation through on-tissue bottom-up or in-source decay in MALDI-MSI: Application to prostate cancer. Anal Bioanal Chem. 2012:1–17.
60. Morgan TM, Seeley EH, Fadare O, Caprioli RM, Clark PE. Imaging the clear cell renal cell carcinoma proteome. J Urol. 2012 S0022–5347(12)04943–9.
61. Hanrieder J, Ljungdahl A, Fälth M, Mammo SE, Bergquist J, Andersson M. L-DOPA-induced dyskinesia is associated with regional increase of striatal dynorphin peptides as elucidated by imaging mass spectrometry. Mol Cell Proteomics. 2011; 10:1–14.
62. Clemis EJ, Smith DS, Camenzind AG, Danell RM, Borchers CH. Quantitation of Spatially-Localized Proteins in Tissue Samples using MALDI-MRM Imaging. Anal Chem. 2012; 84:3514–3522. [PubMed: 22356211]
63. Liu Z, Schey KL. Fragmentation of multiply-charged intact protein ions using MALDI TOF-TOF mass spectrometry. J Am Soc Mass Spectrom. 2008; 19:231–238. [PubMed: 17693096]
64. Hardesty WM, Kelley MC, Mi D, Low RL, Caprioli RM. Protein signatures for survival and recurrence in metastatic melanoma. J Proteomics. 2011; 74:1002–1014. [PubMed: 21549228]
65. Chaurand P, Latham JC, Lane KB, Mobley JA, Polosukhin VV, Wirth PS, Nanney LB, Caprioli RM. Imaging mass spectrometry of intact proteins from alcohol-preserved tissue specimens: Bypassing formalin fixation. J Proteome Res. 2008; 7:3543–3555. [PubMed: 18613713]
66. Grey AC, Gelasco AK, Moreno-Rodriguez RA, Krug EL, Schey KL. Molecular morphology of the chick heart visualized by MALDI imaging mass spectrometry. Anat Rec, Part A. 2010; 293:821–828.
67. Grey AC, Chaurand P, Caprioli RM, Schey KL. MALDI Imaging Mass Spectrometry of Integral Membrane Proteins from Ocular Lens and Retinal Tissue. J Proteome Res. 2009; 8:3278–3283. [PubMed: 19326924]
68. Schey KL, Gutierrez DB, Wang Z, Wei J, Grey AC. Novel fatty acid acylation of lens integral membrane protein aquaporin-0. Biochemistry. 2010; 49:9858–9865. [PubMed: 20942504]
69. Van Remoortere A, Van Zeijl RJM, Van den Oever N, Franck J, Longuespée R, Wisztorski M, Salzet M, Deelder AM, Fournier I, McDonnell LA. MALDI imaging and profiling MS of higher mass proteins from tissue. J Am Soc Mass Spectrom. 2010; 21:1922–1929. [PubMed: 20829063]
70. Franck J, Longuespee R, Wisztorski M, Van Remoortere A, Van Zeijl R, Deelder A, Salzet M, McDonnell L, Fournier I. MALDI mass spectrometry imaging of proteins exceeding 30,000 Da. Med Sci Monit. 2010; 16:BR293–BR299. [PubMed: 20802405]
71. Mainini V, Angel PM, Magni F, Caprioli RM. Detergent enhancement of on-tissue protein analysis by matrix-assisted laser desorption/ionization imaging mass spectrometry. Rapid Commun Mass Spectrom. 2011; 25:199–204. [PubMed: 21157864]

72. Yang J, Caprioli RM. Matrix sublimation/recrystallization for imaging proteins by mass spectrometry at high spatial resolution. Anal Chem. 2011; 83:5728–5734. [PubMed: 21639088]

73. Deutskens F, Yang J, Caprioli RM. High spatial resolution imaging mass spectrometry and classical histology on a single tissue section. J Mass Spectrom. 2011; 46:568–571. [PubMed: 21630385]

74. Oezdemir RF, Gaisa NT, Lindemann-Docter K, Gostek S, Weiskirchen R, Ahrens M, Schwamborn K, Stephan C, Pfister D, Heidenreich A. Proteomic tissue profiling for the improvement of grading of noninvasive papillary urothelial neoplasia. Clin Biochem. 2011; 45:7–11. [PubMed: 21986590]

75. Elsner M, Rauser S, Maier S, Schone C, Balluff B, Meding S, Jung G, Nipp M, Sarioglu H, Maccarrone G. MALDI imaging mass spectrometry reveals COX7A2, TAGLN2 and S100-A10 as novel prognostic markers in Barrett's adenocarcinoma. J Proteomics. 2012; 75:4693–4704. [PubMed: 22365974]

76. Le Faouder J, Laouirem S, Chapelle M, Albuquerque M, Belghiti J, Degos F, Paradis V, Camadro JM, Bedossa P. Imaging mass spectrometry provides fingerprints for distinguishing hepatocellular carcinoma from cirrhosis. J Proteome Res. 2011; 10:3755–3765. [PubMed: 21675781]

77. Attia AS, Schroeder KA, Seeley EH, Wilson KJ, Hammer ND, Colvin DC, Manier ML, Nicklay JJ, Rose KL, Gore JC, Caprioli RM, Skaar EP. Monitoring the Inflammatory Response to Infection through the Integration of MALDI IMS and MRI. Cell Host Microbe. 2012; 11:664–673. [PubMed: 22704626]

78. Trede D, Schiffler S, Becker M, Wirtz S, Steinhorst K, Strehlow J, Aichler M, Kobarg JH, Oetjen J, Dyatlov A. Exploring 3D MALDI imaging mass spectrometry data: 3D spatial segmentation of mouse kidney. Anal Chem. 2012; 84:6079–6087. [PubMed: 22720760]

79. Jones EA, Shyti R, van Zeijl RJM, Ferrari MD, Deelder AM, Tolner EA, van den Maagdenberg AMJM, McDonnell LA. Imaging mass spectrometry to visualize biomolecule distributions in mouse brain tissue following hemispheric cortical spreading depression. J Proteomics. 2012; 75:5027–5035. [PubMed: 22776886]

80. Seeley EH, Caprioli RM. 3D Imaging by Mass Spectrometry: A New Frontier. Anal Chem. 2012; 84:2105–2110. [PubMed: 22276611]

81. Stauber J, Ayed ME, Wisztorski M, Salzet M, Fournier I. Specific MALDI-MSI: Tag-Mass. Methods Mol Biol. 2010; 656:339–361. [PubMed: 20680601]

82. Thiery G, Mernaugh RL, Yan H, Spraggins JM, Yang J, Parl FF, Caprioli RM. Targeted Multiplex Imaging Mass Spectrometry with Single Chain Fragment Variable (scfv) Recombinant Antibodies. J Am Soc Mass Spectrom. 2012; 23:1689–1696. [PubMed: 22869296]

83. Yang J, Chaurand P, Norris JL, Porter NA, Caprioli RM. Activity-Based Probes Linked with Laser-Cleavable Mass Tags for Signal Amplification in Imaging Mass Spectrometry: Analysis of Serine Hydrolase Enzymes in Mammalian Tissue. Anal Chem. 2012; 84:3689–3695. [PubMed: 22424244]

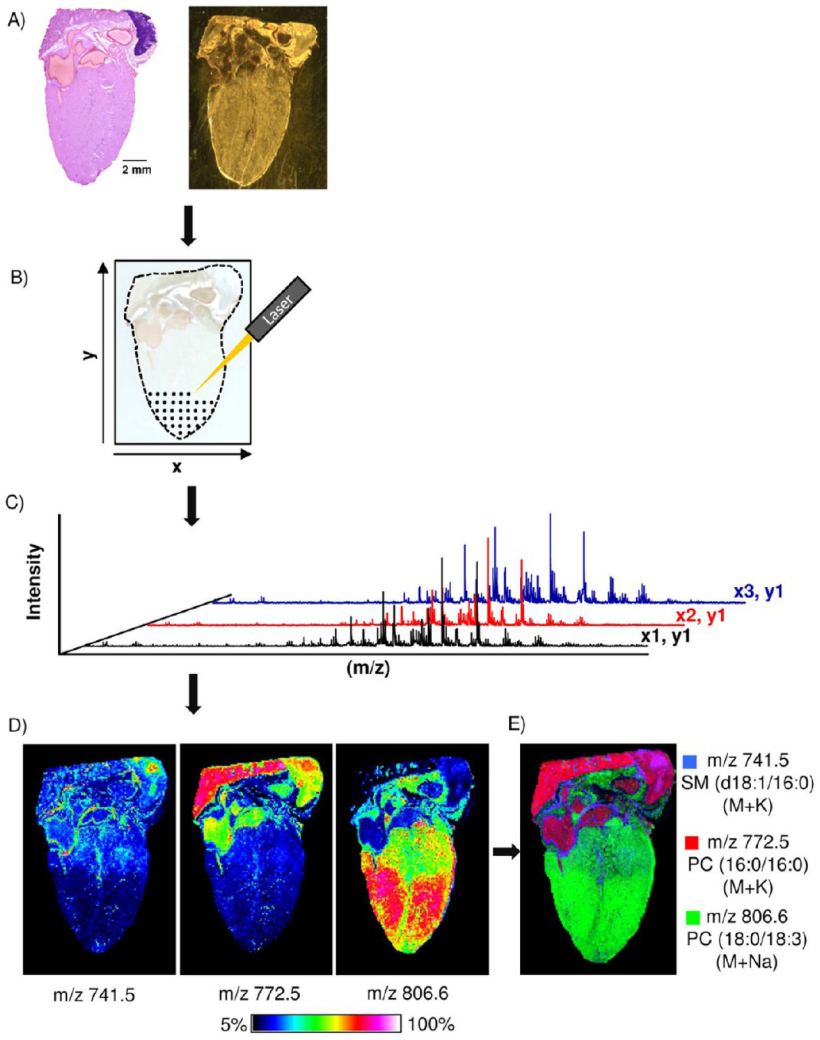

Figure 1.

Overview of an IMS experiment illustrated on a section of adult mouse heart. (A) A fresh frozen section is mounted on a conductive target surface with a serial section used for hematoxylin and eosin (H&E) stain. (B) The matrix is applied by sublimation, and the section is irradiated by the laser in an array pattern. (C) A mass spectrum is generated for each *x*,*y* coordinate. (D) Selected ions are then mapped across the tissue to create images. Images may be combined to form a multiplex ion image. Abbreviations: SM, sphingomyelin; PC, glycerophosphocholine. (E) Images may be combined to form a multiplex ion image.

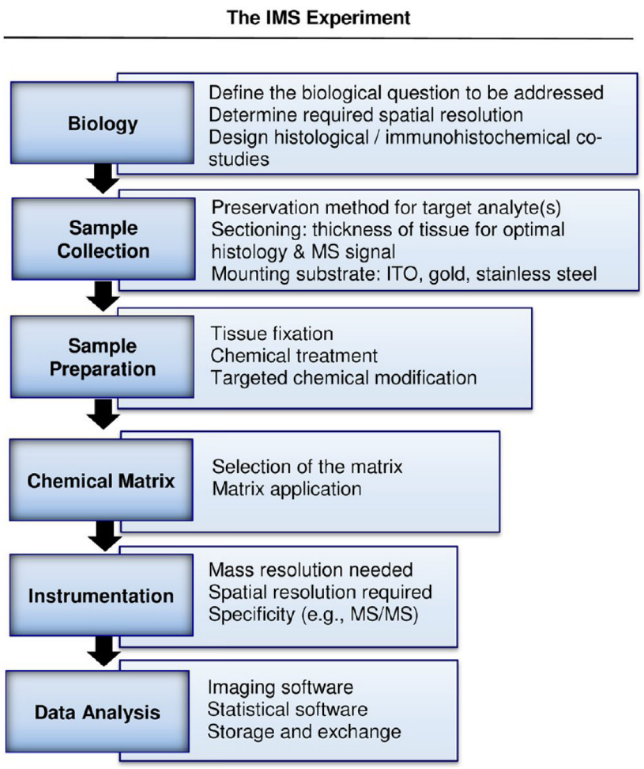

Figure 2.
Experimental workflow that should be considered when designing an IMS experiment.

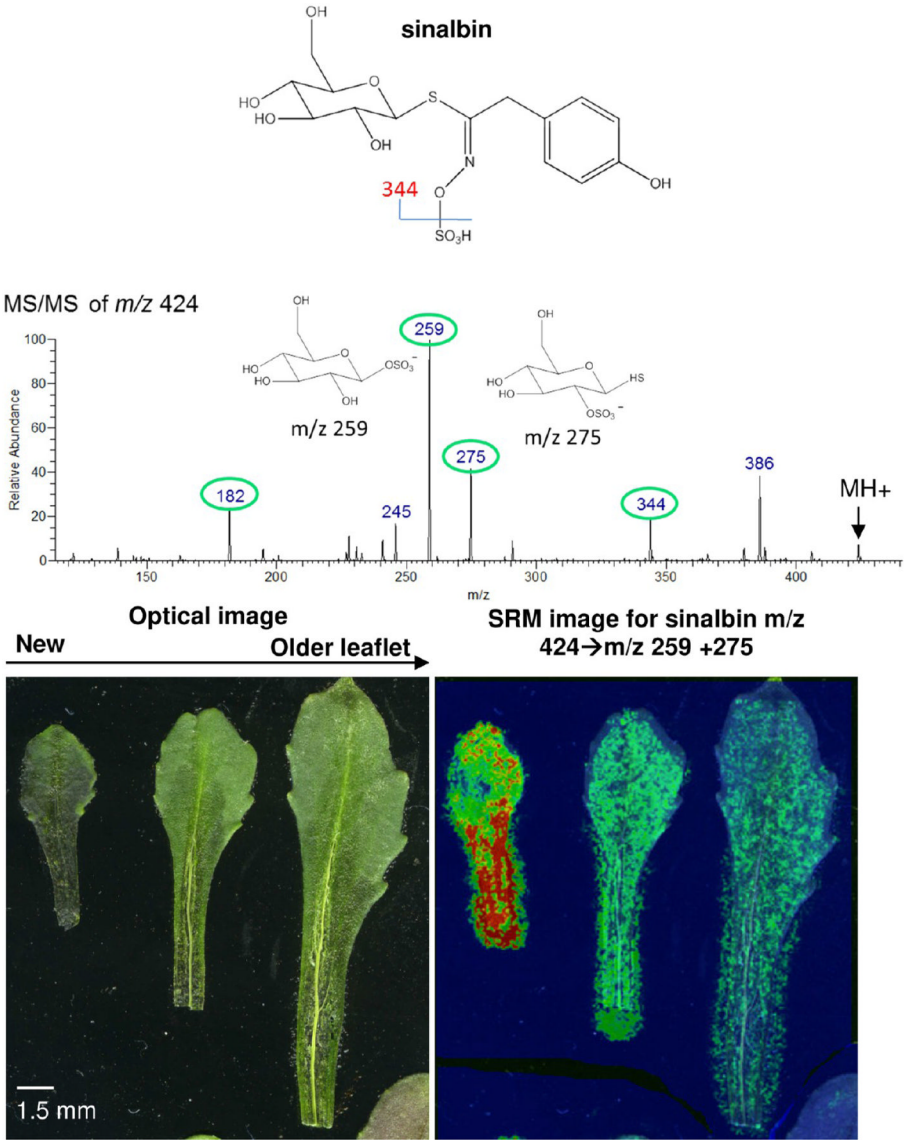

Figure 3.

SRM imaging of sinalbin on *N. caerulescens* on new to older leaflets. The matrix 9-aminoacridine (15 mg/mL in a 9:1 methanol/water mixture) was manually sprayed onto the plant leaf and imaged by MALDI LTQ XL operating in MS/MS mode at a spatial resolution of 100 μm. The image is from the *m*/*z* 424 → *m*/*z* 259 + 275 transition. Sinalbin was detected with a higher concentration in newer leaflets, in agreement with the known protective role of sinalbin in new leaflets. Contributed by M. Reyzer at Vanderbilt University (Nashville, TN) and D. H. McNear at the University of Kentucky (Lexington, KY).

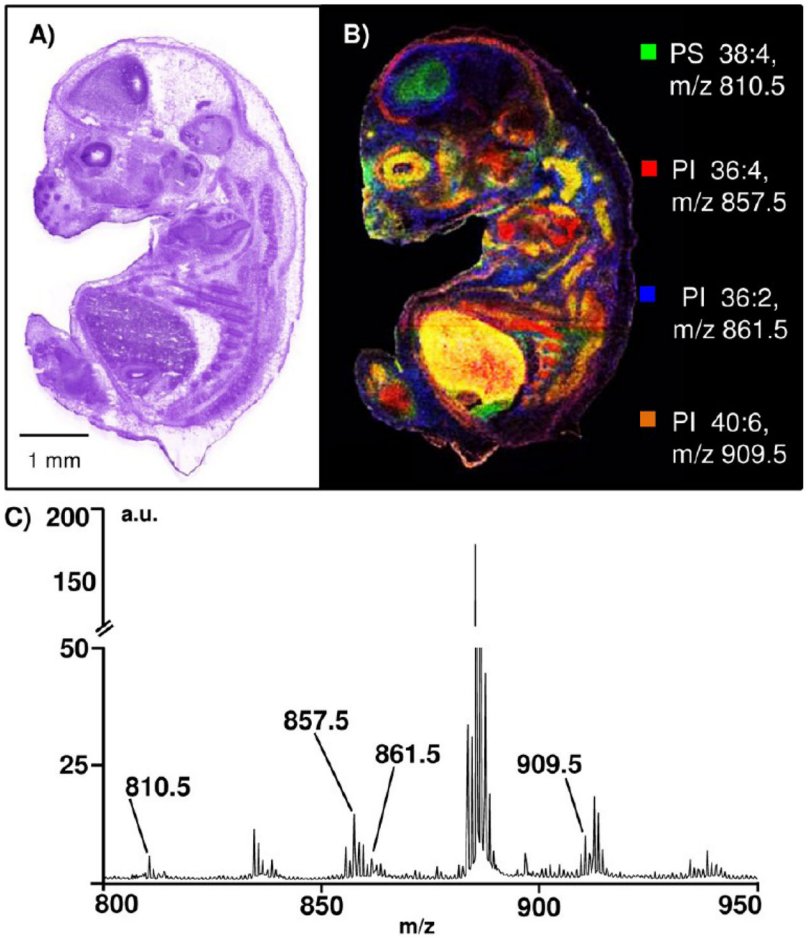

Figure 4.

Combined ion image from four lipids from an imaging experiment on a mouse embryo at embryonic day 13.5. The tissue section was washed with 50 mM ammonium formate, followed by sublimation with DHB. IMS data were collected at a 20 μm spatial resolution in negative ion mode. Lipids are assigned by mass using lipidmaps.com.

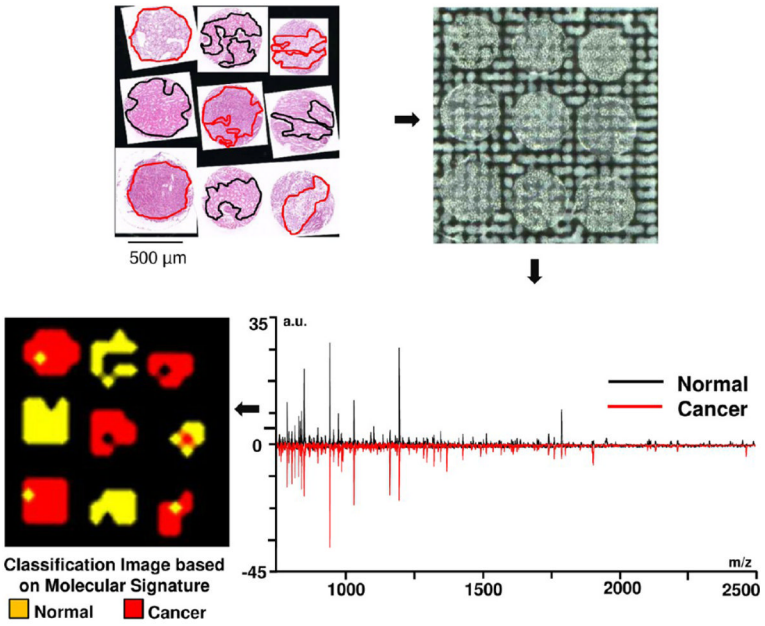

Figure 5.

Peptide imaging illustrated on a portion of a tissue microarray (TMA). The TMA is treated with trypsin, after being mounted on a MALDI target. A pathologist marks an optical image of a serial section stained with H&E as cancer (outlined in red) or normal (outlined in black). This image is then overlaid on the optical image of the TMA prepared for IMS. The TMA is spotted with trypsin, and then matrix and is analyzed by IMS. Marked regions are then compared to formulate molecular signatures that differentiate tumor and normal tissue. A classification model is produced from these signatures for the analysis of additional samples. Here, regions of images that classified as normal are colored yellow, whereas the images that classified as cancer are colored red (image courtesy of E. Seeley and T. Morgan of Vanderbilt University).

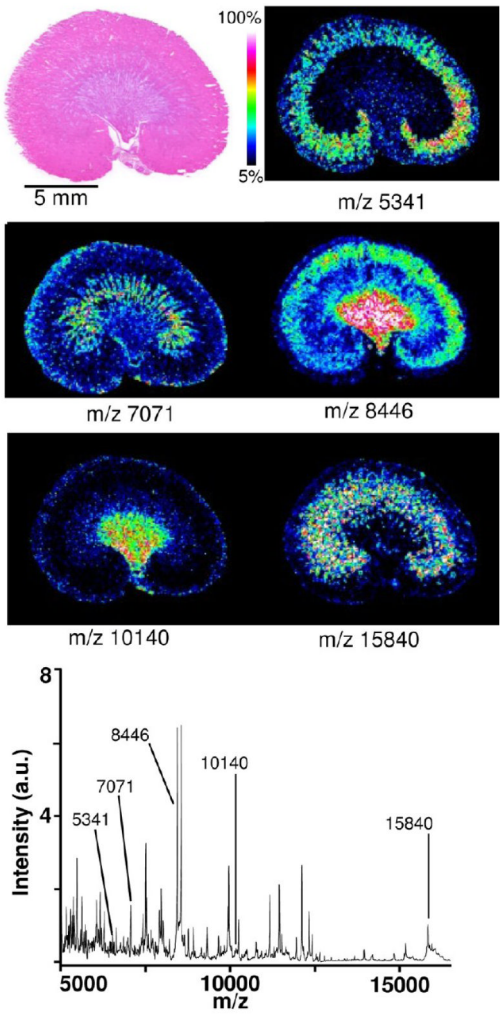

Figure 6.

Protein images from adult rat kidney tissue. Sinapinic acid was applied by sublimation followed by rehydration, and the tissue was imaged at a spatial resolution of 100 μm. Images are shown at 100% of that peak's intensity normalized to total ion current. Image contributed by J. Yang of Vanderbilt University.